Robotic Autonomous Outdoor Gamma Radiation Monitoring and Mapping

Tomas Jilek, Ludek Zalud, and Petra Kocmanova

***Abstract*—**The paper deals with fully autonomous gamma radiation measurement in light outdoor terrain with use of advanced robotic system. Gamma-radiation distribution field experiments made for SURO v.v.i. Czech governmental protection institution are described in the paper. The experiment setup as well as Orpheus-X4 robotic system used in the experiments are described. Algorithms to autonomously navigate the robot in predefined area based on high-precision GNSS (Global Navigation Satellite System) are presented. Examples of radiation maps acquired in secured area during experiments with high-precision position measurement are presented and compared to the data from standard-precision GPS.

***Keywords*—**autonomous navigation, gamma radiation, robot, robotic reconnaissance

I. Introduction

Reconnaissance mobile robotics gains importance during the last years. There are many missions in today's society that may require expendable robots to perform exploration in inaccessible or dangerous environments instead of indispensable people, e.g. CBRNE (Chemical, biological, radio-logical, nuclear, explosive), counter-terrorist fight, US&R (Urban Search and Rescue), etc.

One of promising applications is outdoor radiation distribution measurement. The high demand for exclusion of people from direct measurement is obvious – radiation is not directly observable by people, but it may be extremely dangerous for our life. The radiation impact to our bodies is somewhat cumulative, so even for experiments and/or practical missions with relatively low radiation levels it is reasonable to minimize the human exposition. The situation is similar or in many aspects identical for chemical and/or biological contamination measurements, so mostly the same equipment and similar algorithms may be used.

It is typical to construct one combined vehicles or devices indicated as CBRN. See Figure 1 and 2 for example of relatively universal CBRN robot developed by our team. Orpheus-AC2 robot is extremely rugged machine, but its main drawback is that it is solely teleoperated robot. So the operator has to be in the reach of the robot-to-vehicle communication device and has to control the robot in real-time during the whole mission. This approach is very profitable for several missions, like primary contamination measurement in potentially heavily contaminated areas with other possible risks (explosives, antagonist opposition, etc.), but has its limits in other missions, where bigger area of interest with typically lower radiation levels has to be examined.

The aim of our team is now to develop autonomous exploration/measurement in predefined area. Since this task is, in general, extremely ambitious, we decided to restrict it to well defined, unstructured outdoor environments, like meadows, agricultural fields, etc. The idea is that the operator defines four outlaying points in the field, the separation among measurements is defined, and the robot automatically calculates the path and makes the measurement fully autonomously. For robot precise self-localization, RTK (Real-Time Kinematics)-GNSS is used. The same data are used also for logging of position and radiation data with corresponding time-stamp during measurement.

Fig. 1 Orpheus-AC2 military robot for CBRN operator-controlled reconnaissance – the robot (left), operator's station inside the armored car (right)

This work was supported by VG 2012 2015 096 grant named Cooperative Robotic Exploration of Dangerous Areas by Ministry of Interior, Czech Republic, program BV II/2-VS.

This work was supported by the project CEITEC – Central European Institute of Technology (CZ.1.05/1.1.00/02.0068) from the European Regional Development Fund and by the Technology Agency of the Czech Republic under the project TH01020862 "System for automatic/automated detection/monitoring radiation situation and localization of hot spots based on a smart multifunctional detection head usable for stationary and mobile platforms incl. unmanned".

L. Zalud is with the LTR s.r.o., Brno, Czech Republic (e-mail: zalud@orpheus-project.cz, web: http://www.orpheus-project.cz) and with Central European Institute of Technology, Brno University of Technology, Brno, Czech Republic (phone: 00420541146416; e-mail: ludek.zalud@ceitec.vutbr.cz).

T. Jilek is with the LTR s.r.o., Brno, Czech Republic and with the Central European Institute of Technology, Brno University of Technology, Brno, Czech Republic (e-mail: tomas.jilek@ceitec.vutbr.cz).

P. Kocmanova is with the Central European Institute of Technology, Brno University of Technology, Brno, Czech Republic, (e-mail: petra.kocmanova@ceitec.vutbr.cz).

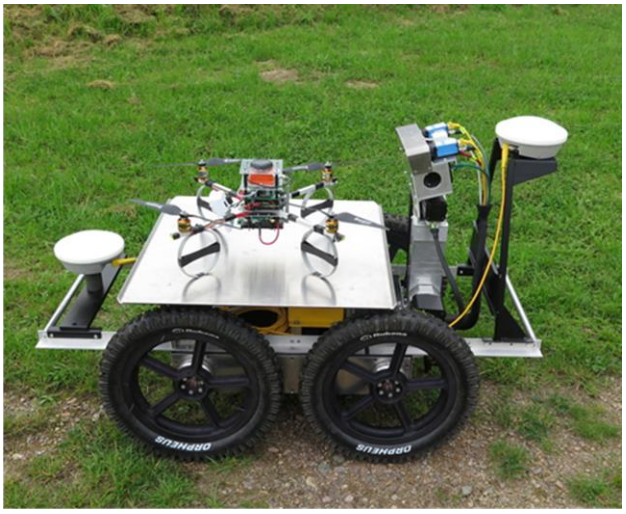

Fig. 2 Orpheus-AC2 military robot for CBRN operator-controlled reconnaissance, robot-retaining system detail

II. System Description

The aim of this chapter is to describe the system that was used during the two experiments described in the next chapter.

Our team is highly involved in development of extremely durable robots for contaminated areas. We have developed three different mid-size robots (approx. 50 kg) for both military and non-military missions in potentially contaminated areas. They are called Orpheus-AC-P, Orpheus-AC, and Orpheus-AC2 [7], [11]. These robots passed through 18 MIL-STD tests, including their ability to withstand contamination and decontamination. Although they might seem ideal for such an application, for several reasons we were not able to use these robots during the hereinafter described experiments. We had to use non-military robot Orpheus-X4 that is not prepared for contamination, but is very flexible when mechanical and electronics modifications have to be done, as in our case.

A. Orpheus-X4

Orpheus-X4 [8], [9], [10], [12] is non-military robot belonging to the same generation as Orpheus-AC2. The main parameters of Orpheus-X4 robot are in Table 1.

Table 1 Orpheus-X4 parameters

Parameter	Value
Dimensions (l × w × h)	950 × 585 × 709 mm
Weight	56 kg
Operation time	90 minutes
Drive type	differential
Maximum speed	12 km/h

For the first experiment, the robot was covered by plastic bags to be protected against possible contamination by the radioactive dust. The robot was carefully scanned for radiation after the experiment.

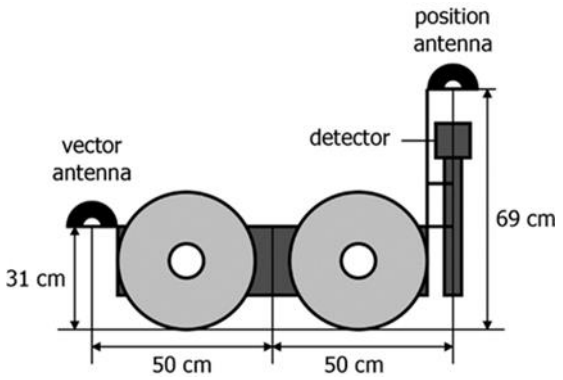

Fig. 3 Orpheus-X4 with Uranus drone photo (up), sensor and antennas placement during the experiments (down)

The robot construction was modified for the experiments. The sensory head was not used, so it was deactivated. Trimble embedded RTK GNSS with two antennas was used for precise navigation and measurement. Custom made scintillation gamma-radiation probe with precise time derived from on-device GPS receiver, connected to data logger was used to measure radiation intensity. Since these devices are relatively large and must be exactly and rigidly placed on the robot, we developed custom metal frame. The main advantage is placement of the main antenna above the radiation sensor – that means the position data for radiation data-logging do not need to be recalculated – height is not considered, since it is supposed to be equal during the experiment (see Figure 3).

B. Trimble RTK GNSS receiver

Two Trimble BX982 RTK GNSS receivers were used for precise position and orientation measurement of Orpheus-X4 robot during the experiments. One of them was used as stationery base-station, the other one was used onboard the robot in rover configuration.

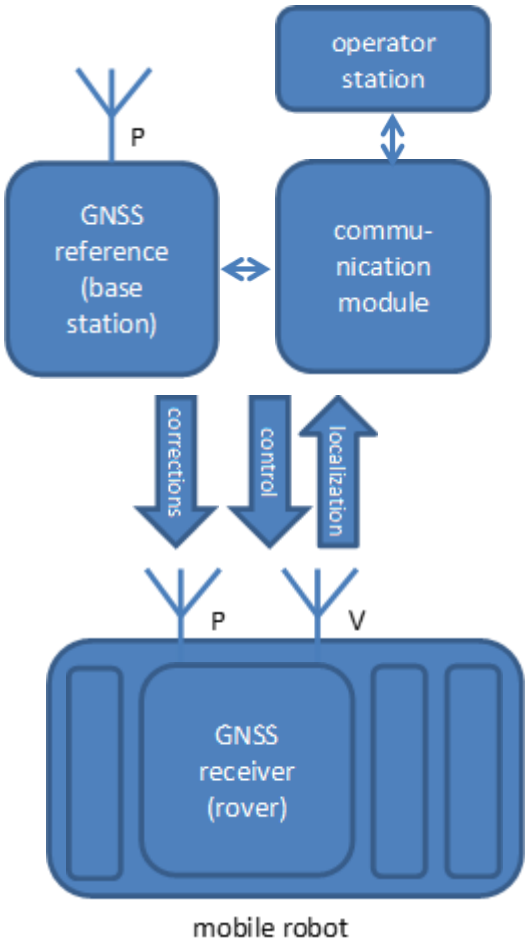

Fig. 4 GNSS configuration. P – position antenna, V – vector antenna

Table 2 Trimble BX982 embedded GNSS receiver main parameters [1]

Parameter	Value
Number of channels	220
GNSS	GPS, GLONASS
RTK solution	supported
Dual antenna	supported
Power	9 – 28 V (5 W max.)
Weight	1.6 kg
Size	264 × 140 × 55 mm
Operating temperature	-40 °C – +70 °C

The GNSS measurement configuration is on Figure 4. Although we used two identical modules, their configuration was different. The module named as *base station* contained only one antenna input, and the main module used is RTK BASE. The other embedded module on the other hand had the dual-input enabled, as well as RTK ROVER. The calculation frequency on both modules was 50 Hz.

Fig. 5 Orpheus robot during the first experiment. Vital parts were covered by plastic bags as radiation dust protection (up); the robot has to be measured and eventually decontaminated (down).

The robot GNSS was used also for azimuth measurement in double-antenna configuration. As it is visible from Figure 5, the antennas were not placed in the same height. The reason was purely practical – we decided to place the main antenna above the radiation detector, so the latitude and longitude coming from it corresponds approximately to the ones of the sensor. Inaccuracy caused by robot tilting can be omitted for this application. Although this feature is not well documented, the GNSS is able to calculate both precise position and orientation even if the antennas are not in the same height.

Certain amount of data has to be transmitted from base-station to the data to achieve RTK solution. The data were transmitted through our custom micro-wave datalink that is able to transfer up to 1 Mbit/sec. The datalink was used for several other purposes, like remote control of the robot in manual mode, remote control of the auto-mode system parameters and inspection, during the experiment. The necessary communication reach was about 200 meters in our case, what was well suited for our datalink. If necessary the communication datalink may be substituted by other technologies, since the physical connection coming from our robot may vary from Ethernet, to CAN or RS 232/485. So the communication with the robot may be easily extended.

III. Path Planning and Navigation

Path-planning and navigation algorithms for autonomous

robot navigation are described in the following sections.

A. Waypoint Calculation

The complete path planning algorithm may be described as follows (see Figure 6).

1. Four points A, B, C, D surrounding the area of interest have to be defined manually.
2. The area is divided into defined number of sections in two axis defined by points AB, AC.
3. Numbered array of waypoints is calculated.

When the numbered waypoint network is defined, the robot can traverse them in corresponding order.

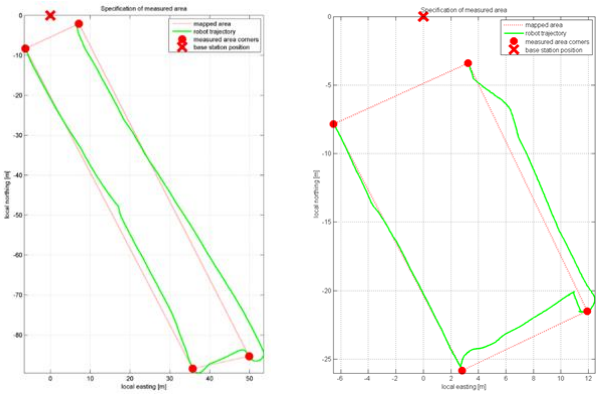

Fig. 6 Area of interest definition – demonstrated on data from the second experiment

B. Robot Navigation

Calculation using rhumb line is used for recalculation the measured GNSS main antenna position coordinates to the point lying in the robot rotation axis.

$$\varphi_c = \varphi_m - \frac{l_a}{r_e}\cos\theta, \tag{1}$$

$$\lambda_c = \lambda_m - \left(\ln\left(\tan\left(\frac{\varphi_m}{2}+\frac{\pi}{4}\right)\right) - \ln\left(\tan\left(\frac{\varphi_c}{2}+\frac{\pi}{2}\right)\right)\right)\tan\theta, \tag{2}$$

where φ_c, φ_m – latitude recalculated, measured, l_a – distance between antenna and rotation axis in horizontal plane, r_e – substitute sphere radius, λ_c, λ_m – longitude recalculated, measured, θ – azimuth of mobile robot.

Block scheme of the used navigation method is on Figure 7. In the first block the navigation solution is calculated based on waypoint sequence and current mobile robot position (vector p_R) and orientation (vector o_R).The output from this solution represents the maximum allowed forward speed ($v_{R,lim}$) and regulation error (β_R) of mobile robot azimuth. Based on these variables, parameters of acquired mobile robot movement, such as forward speed v_R^s and angular speed ω_R^s, that are independent on individual drive configuration, are calculated. These variables are than transformed to control variables according to the currently used drive configuration. They are represented by vector ω_m^s (motor rotation speeds) and angles γ_a^s (individual wheel left-to-right steering), if they are used. State information about mobile robot position and orientation measured by RTK GNSS is fed to the feedback.

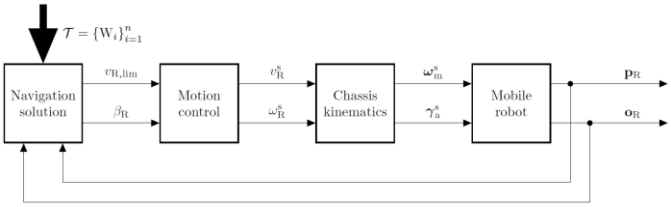

Fig. 7 Block scheme of the navigation method

In Figure 8 the data-processing flow in navigation solution block is depicted in more detail. Based on the current mobile robot position [λ_R, φ_R] and current navigation point position [λ_N, φ_N] the navigation curve parameters are calculated. They are initial azimuth α_{RN} and length l_{RN}. Regulation error of mobile robot azimuth is calculated from the difference between initial azimuth of navigation curve and current effective mobile robot azimuth. This quantity is normalized to the range -180° to +180°. If very high accuracy of waypoint traversal is required, the forward speed limit is decreased when nearby the actual waypoint.

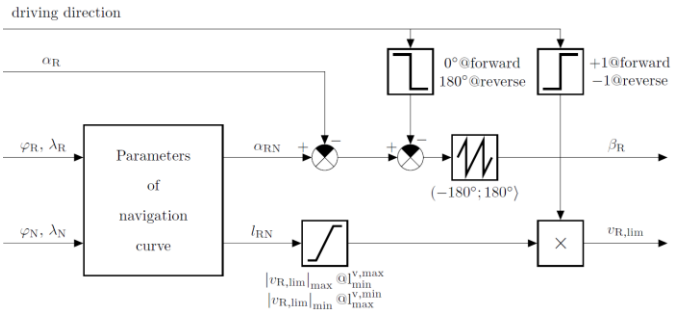

Fig. 8 Data processing in navigation solver

In *Motion Control* block the forward speed of mobile robot during its turn is limited. It is done according to the selected speed limit (see Figure 9). If the control deviation is low, the speed is not decreased. Turning of the mobile robot is given by angular speed of its movement. Transfer function of the used proportional controller for azimuth control is on Figure 10.

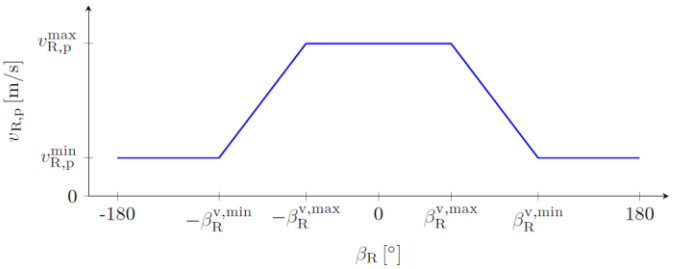

Fig. 9 Speed profile of forward speed

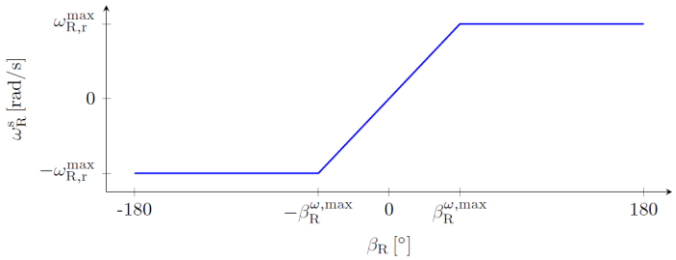

Fig. 10 Transfer characteristics of the used azimuth controller

C. *Required parameters of navigation point*

In the beginning of each navigation cycle it is necessary to get the coordinates of the actual navigation point for which the navigation solution will be calculated. The navigation point must fulfill the following conditions:

1. The point has to be in the so far not traversed trajectory part.
2. The point must fulfill the minimum distance from the mobile robot.
3. The point must be accessible under the curvature diameter that fulfills the constraints of the used drive configuration.
4. The point ensures convergention of the real trajectory to the desired trajectory.

D. *Kinematic solution*

Parameters of the requested movement are transformed to required individual wheel angular drive speed (see Equation 3). Kinematic model of the used drive configuration is in Figure 11.

$$\omega_{m,i}^s = f\left(v_R^s, \omega_R^s\right) \tag{3}$$

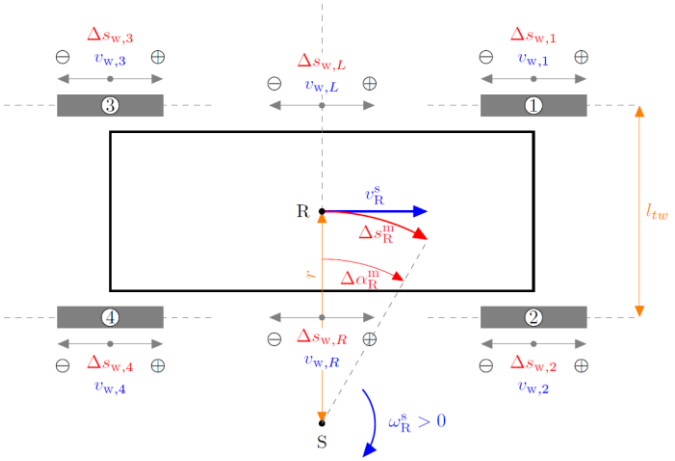

Fig. 11 Kinematic model of skid-steer driven drive

Vector $\omega_m{}^s$ of controlled motor speeds is determined by Equation 4.

$$\boldsymbol{\omega}_m^s = \begin{pmatrix} \left(v_R^s + \frac{1}{2}\xi\omega_R^s\right)c_{w,1} \\ \left(v_R^s + \frac{1}{2}\xi\omega_R^s\right)c_{w,2} \\ \left(v_R^s + \frac{1}{2}\xi\omega_R^s\right)c_{w,3} \\ \left(v_R^s + \frac{1}{2}\xi\omega_R^s\right)c_{w,4} \end{pmatrix} \tag{4}$$

Individual constants $c_{w,i}$ include relevant wheel parameters (gear ratio, wheel perimeter, …). Values of these constants for the currently used platform are acquired by calibration process. Quantity ξ corresponds to the effective track width and is calibrated for all used forward and angular speeds of the mobile robot.

IV. Experiments

Two practical experiments were done with the described equipment. The experiments were done as cooperation between SURO v.v.i. and Brno University of Technology.

A. *Ground radioactive contamination measurement experiment*

The aim of the first experiment was to measure radiation caused by La-140 isotope dust spread on grass-covered meadow.

In this experiment the robot was controlled remotely by operator in real-time, so the autonomous movement was not used. RTK GNSS technique was only used for precise position data-logging.

The results of the experiment are positive – it proved the use of Orpheus robotic system for remote radiation measurement is possible and profitable.

The experiment also proved it would be extremely profitable to have fully autonomous robot movement during the experiment – both for higher precision of the path and to be more considerate to the mechanical parts of the robot.

B. *Lost radiation sources experiment*

The second experiment was somewhat different. The main idea was to localize randomly located sealed radiation sources.

The main difference from technical point of view was use of the fully autonomous path-planning and navigation, as described in Chapter III.

Two measurements were done – one on greater area and one on smaller (see Figure 6) to be able to test influence of more dense data on explanatory value of the experiment.

Table 3 Large area surrounding polygon

Point	Point	Distance [m]	Division [-]	Span [m]
A	D	14.8	15	0.99
B	C	14.5	15	0.97
A	B	90.5	18	5.03
C	D	93.6	18	5.20

Table 4 Small area surrounding polygon

Point	Point	Distance [m]	Division [-]	Span [m]
A	D	10.7	10	1.07
B	C	10.1	10	1.07
A	B	20.3	20	1.01
C	D	20.1	20	1.00

The measurement was performed on grass-covered meadow nearby Trebic, Czech Republic. The area of interest (points A, B, C, D – see Figure 6) was marked by the robot controlled manually, the division to appropriate parts was done automatically by hereinbefore described algorithms to form approximately 1 m × 5 m rectangles in the first case (see Table 3) and approximately 1 m × 1 m in the second case (see Table 4).

The resulting network with automatically generated waypoints is on Figure 12 left and right, and Figure 14 left and right. The resulting intensity map is on Figure 13 and Figure 15.

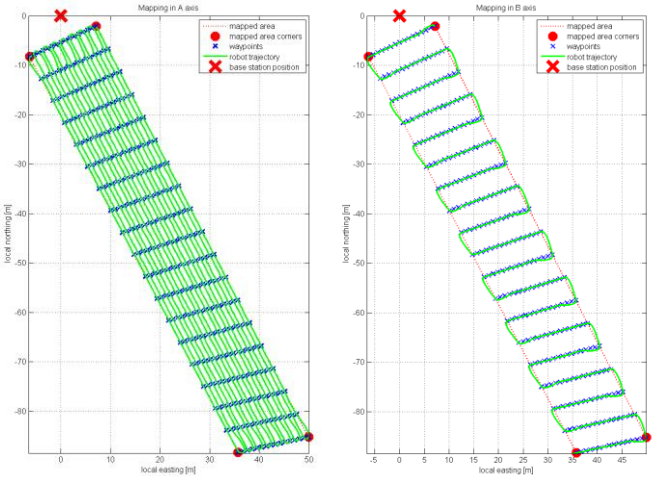

Fig. 12 Results – large area; horizontal (left) and vertical (right) span with waypoints and real traversed trajectory

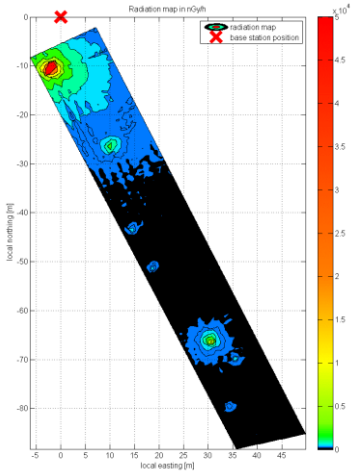

Fig. 13 Results – large area; intensity map

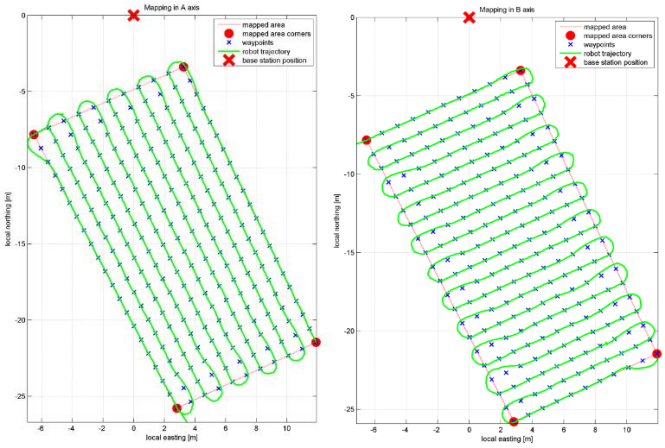

Fig. 14 Results – small area; horizontal (left) and vertical (right) span with waypoints and real traversed trajectory

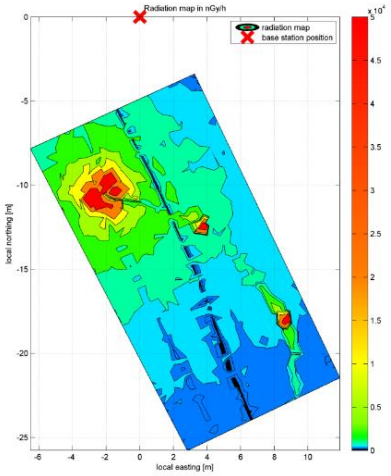

Fig. 15 Results – small area; intensity map

V. Conclusion

The main aim of this article was to demonstrate the possibility of fully autonomous monitoring, measurement and mapping of contaminated areas through mobile robot. As a demonstration, gamma radiation measured by Orpheus-X4 robot was taken, but the applications are not limited to this robot and this type of radiation only. CBRN threats are becoming more serious problem during last years, mainly due to higher terrorist activity and asymmetrical war conflicts, and this approach may help in most of them. Robotic measurement in contaminated areas is more safe and far more precise and reliable than the one performed by people. The same algorithms may be also used in environmental protection application in our ordinary life. The robots may for example guard around certain facilities with chemical or other contamination risks, while still providing other security-related functions - e.g. guard against hostiles, make thermal images to prevent fire and/or technological issues, etc. Contrary to people the robot will never be exhausted, even if it is hit by high amount of radiation, it will more likely sustain it and even if not, its value is definitely lower than the one of human beings.

As it is visible on the results from our experiments on Figure 13 right, and Figure 15 right, the measurements were successful. It is obvious the autonomous path-planning, waypoint generation and navigation using precise RTK GNSS helped a lot to acquire consistent data. It also minimizes potential risk of operator error causing the measurement might be completely useless due to small part not being traversed and measured.

The same RTK GNSS complete was used for two different tasks in the second experiment – precise time and position data logging and robot navigation.

The original idea provided by the customer was to use classical GPS that is onboard the scintillation radiation sensor. Instead we proposed and designed system that relies on RTK GNSS with substantially higher precision. The result may be easily compared from Figure 15 and Figure 16. The later graph demonstrates the same measurement based on data from the named low-resolution non-RTK GPS.

The resulting gamma-radiation diagram aligned with aerial photo is on Figure 17.

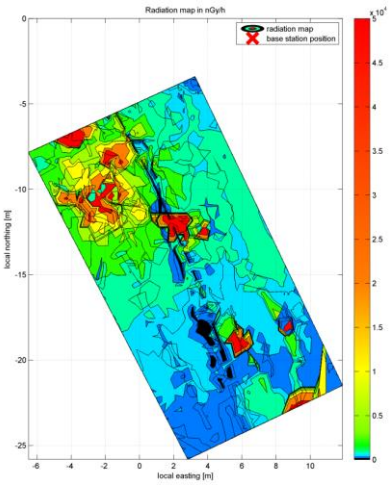

Fig. 16 Demonstration of intensity map based on data from standard L1 GPS with code based measurement only

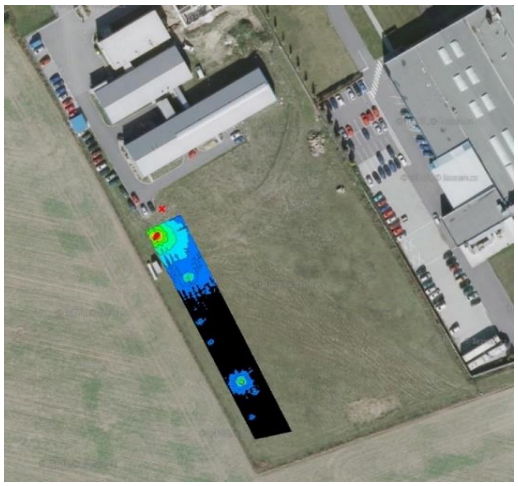

Fig. 17 Resulting gamma-radiation intensity map in aerial photo

REFERENCES

[1] Trimble BX982 datasheet. (12. 12. 2014). [Online]. Available: http://www.dpie.com/datasheets/gps/Trimble-BX982-Datasheet-Document-581007.pdf

[2] Leica FPES Flight Planning & Evaluation Software. (15. 12. 2014). [Online]. Available: http://www.leica-geosystems.be/downloads123/zz/airborne/fpes/brochures/Leica_FPES_BRO.pdf

[3] T. M. Driscoll, *Complete coverage path planning in an agricultural environment*, Iowa State University, Graduate Thesis, 2011. (5.12.2014). [Online]. Available: http://lib.dr.iastate.edu/cgi/viewcontent.cgi?article=3053&context=etd

[4] I. A. Hameed, *Intelligent Coverage Path Planning for Agricultural Robots and Autonomous Machines on Three-Dimensional Terrain*, Journal of Intelligent Robot Systems, Springer, 2012

[5] S.W. Moon, D. H. Shim, *Study on Path Planning Algorithms for Unmanned Agricultural Helicopters in Complex Environment*, International Journal of Aeronautical and Space Science, 2009, vol. 10. No. 2.

[6] H. Eisenbeiss, Applications of photogrammetric processing using an autonomous model helicopter, *symposium ISPRS Commission Technique I "Des capteurs a l'Imagerie"*, n185, 2007

[7] L. Zalud, F. Burian, L. Kopecny, and P. Kocmanova, "Remote Robotic Exploration of Contaminated and Dangerous Areas", in *International Conference on Military Technologies*, pp 525-532, Brno, Czech Republic, ISBN 978-80-7231-917-6, 2013.

[8] L. Zalud and P. Kocmanova, "Fusion of thermal imaging and CCD camera-based data for stereovision visual telepresence", in 2013 IEEE *International Symposium on Safety, Security, and Rescue Robotics (SSRR)*. Linkoping: IEEE, 2013, pp. 1-6. DOI: 10.1109/SSRR.2013.6719344. ISBN 978-1-4799-0880-6

[9] P. Kocmanova, A. Chromy, L. Zalud, "3D Proximity Laser Scanner Calibration", in 2013 18th international conference on methods and models in automation and robotics (MMAR), pp 742-747, ISBN 978-146735506-3,

[10] L. Nejdl, J. Kudr, K. Cihalova, et. al. "Remote-controlled robotic platform ORPHEUS as a new tool for detection of bacteria in the environment", in ELECTROPHORESIS, Volume: 35 Issue: 16 , Special Issue: SI, Pages: 2333-2345, 10.1002/elps.201300576

[11] L. Zalud, L. Kopecny, F. Burian, "Robotic Systems for Special Reconnaissance", International Conference on Military Technologies, pp 531-540, Brno, Czech Republic, ISBN 978-80-7231-649-6, Oprox, 2009

[12] Chromy, A., Zalud, L. "Robotic 3D scanner as an alternative to standard modalities of medical imaging", (2014) SpringerPlus, DOI: 10.1186/2193-1801-3-13